

## Two-body quantum propagation in arbitrary potentials

This content has been downloaded from IOPscience. Please scroll down to see the full text.

2016 J. Phys.: Conf. Ser. 738 012028

(<http://iopscience.iop.org/1742-6596/738/1/012028>)

View [the table of contents for this issue](#), or go to the [journal homepage](#) for more

### Download details:

IP Address: 82.48.146.204

This content was downloaded on 08/09/2016 at 14:22

Please note that [terms and conditions apply](#).

You may also be interested in:

[Nucleon Two-Body Decay and the Related Bound State Effects](#)

Chao-hsi Chang and Yong-shi Wu

[Two-Body Scattering in \(1 plus 1\) Dimensions by a Semi-relativistic Formalism and a Hultheacuten Interaction Potential](#)

S. Hassanabadi, M. Ghominejad and K.-E. Thylwe

[Uranium ions stripped bare](#)

Jean Pierre Briand

[Three-body entanglement induced by spontaneous emission in a three two-level atoms system](#)

Liao Xiang-Ping, Fang Mao-Fa, Zheng Xiao-Juan et al.

[A unitary and relativistic model for  \$\pi\$  and  \$\eta\$  photoproduction](#)

Alvin Kiswandhi, Simon Capstick and T-S H Lee

[Dalitz plot analysis in the FOCUS experiment](#)

Sandra Malvezzi and the FOCUS Collaboration

# Two-body quantum propagation in arbitrary potentials

Federico Grasselli<sup>1,2</sup>, Andrea Bertoni<sup>2</sup>, and Guido Goldoni<sup>1,2</sup>

<sup>1</sup>Dipartimento di Scienze Fisiche, Informatiche e Matematiche, Università degli Studi di Modena e Reggio Emilia, Via Campi 213/a, Modena, Italy

<sup>2</sup>S3, Consiglio Nazionale delle Ricerche, Istituto Nanoscienze, Via Campi 213/a, Modena, Italy

E-mail: federico.grasselli@unimore.it

**Abstract.** We have implemented a unitary, numerically exact, Fourier split step method, based on a proper Suzuki-Trotter factorization of the quantum evolution operator, to propagate a two-body complex in arbitrary external potential landscapes taking into account exactly the internal structure. We have simulated spatially indirect Wannier-Mott excitons – optically excited electron-hole pairs with the two charges confined to different layers of a semiconductor heterostructure with prototypical 1D and 2D potentials emphasizing the effects of the internal dynamics and the insufficiency of mean-field methods in this context.

## 1. Introduction

When a composite object, say two attracting particles, is dynamically propagated, its internal structure cannot be *a priori* neglected, and energy might be transferred between the relative motion and the centre-of-mass (c.m.) degrees of freedom (DOFs) by an external one-body potential acting on the each particle separately. In the quantum regime, electron-hole correlations or, equivalently, c.m.–relative motion correlations must be carefully included even if the c.m. kinetic energy is not sufficient to excite any internal transition. In particular, mean-field approximations, neglecting dynamical correlations by construction, produce propagations which in general differ substantially from exact calculations.[1]

In this paper we discuss the exact unitary propagation in selected 1D and 2D configurations of a spatially indirect Wannier-Mott exciton (IX) in a GaAs-based semiconductor double-quantum-well (QW) heterostructure, i.e., a photogenerated electron-hole (*e-h*) pair in which the two charges are kept separated to different layers.

## 2. Theoretical model and quantum evolution algorithm

In the absence of external potential landscapes, the two-particle Hamiltonian reads

$$H_0 = -\frac{\hbar^2}{2M}\nabla_{\mathbf{R}}^2 - \frac{\hbar^2}{2m}\nabla_{\mathbf{r}}^2 + U_{\text{int}}(\mathbf{r}) \quad (1)$$

where  $\mathbf{R} \equiv (m_1\mathbf{r}_1 + m_2\mathbf{r}_2)/M$ , and  $\mathbf{r} \equiv \mathbf{r}_1 - \mathbf{r}_2$  are the c.m. and relative coordinates, respectively,  $M \equiv m_1 + m_2$  and  $m \equiv (m_1^{-1} + m_2^{-1})^{-1}$  being the total and reduced masses of the system, respectively.  $U_{\text{int}}(\mathbf{r})$  is the interaction attractive potential of the two particles,<sup>1</sup> giving a set of

<sup>1</sup> It is in principle not necessary the stricter dependence of  $U_{\text{int}}$  on the *modulus* of  $\mathbf{r}$  in our propagation method.



bound states  $\phi_n(\mathbf{r})$ , with eigenenergies  $\epsilon_n$ , for the two-body internal dynamics. The c.m. and relative coordinate representation, which is separable in the absence of an external potential, is particularly convenient. First, a single-particle external potential, acting on the two particles at positions  $\mathbf{r}_1, \mathbf{r}_2$ , can be written as  $U_{\text{ext}} = U_1(\mathbf{r}_1) + U_2(\mathbf{r}_2) = U_{\text{ext}}(\mathbf{R}, \mathbf{r})$ , and in general breaks the separability of the exciton Hamiltonian: when  $U_{\text{ext}} \neq 0$ , we must deal with a general  $(2 \times D)$ -DOF problem, where  $D$  is the dimensionality. If, however,  $U_{\text{ext}}$  is not strong enough to dissociate the electron-hole pair, the relative coordinate  $\mathbf{r}$  remains in a finite region about  $\mathbf{r} = 0$ . Therefore, for numerical propagation, the c.m. and relative coordinates representation is particularly convenient compared to formally equivalent  $\mathbf{r}_1, \mathbf{r}_2$  representation.

In order to obtain the coherent quantum dynamics of the total wave function of the two-body complex,  $\Psi = \Psi(\mathbf{R}, \mathbf{r}; t)$ , we have to solve the time-dependent Schrödinger equation (TDSE). This can be done numerically by repeated application of the evolution operator,  $\mathcal{U}(t, t + \Delta t)$ , between times  $t$  and  $t + \Delta t$ , as

$$\Psi(\mathbf{R}, \mathbf{r}; t + \Delta t) = \mathcal{U}(t + \Delta t; t)\Psi(\mathbf{R}, \mathbf{r}; t). \quad (2)$$

We adopt the following Suzuki-Trotter factorization for  $\mathcal{U}$ : [2]

$$\mathcal{U}(t + \Delta t; t) = e^{-\frac{i}{\hbar}U_{\text{tot}}\frac{\Delta t}{2}} e^{-\frac{i}{\hbar}T\Delta t} e^{-\frac{i}{\hbar}U_{\text{tot}}\frac{\Delta t}{2}} + O(\Delta t^3). \quad (3)$$

Here  $T = \mathbf{P}^2/(2M) + \mathbf{p}^2/(2m)$  is the total kinetic energy operator, where  $\mathbf{P}$  and  $\mathbf{p}$  are c.m. and relative momenta, respectively, and  $U_{\text{tot}} = U_{\text{int}}(\mathbf{r}) + U_{\text{ext}}(\mathbf{R}, \mathbf{r})$  is the total potential energy operator. The evolution operator is thus the product of terms, each diagonal either in direct or in reciprocal space (see Appendix in Ref. [3] for details). Therefore, by switching from position to momentum representation, and *vice versa*, through Fourier transformation, the application of  $\mathcal{U}$  on  $\Psi$  reduces to simple array-by-array multiplication. This, and the use of fast Fourier transform algorithms, results in higher computational efficiency compared to other TDSE solvers, like those based on finite difference discretized Hamiltonian (e.g. the Crank-Nicolson method). This method is called the Fourier split step approach. [4, 5]. It is unitary, numerically exact as  $\Delta t \rightarrow 0$ , and straightforwardly applicable to time dependent potentials. Also, it can be parallelized for massively parallel architectures.

Below we discuss the exact propagation of an indirect IX under different external potentials in 1D, [3] and 2D. [1] In all cases, we chose the initial state of the simulation as the product  $\Psi(\mathbf{R}, \mathbf{r}; t = 0)$  of a c.m. Gaussian of width  $\sigma$ , centred at  $\mathbf{R}_0$ , and propagating with central wave vector  $\mathbf{K}_0$ ,  $\chi_G(\mathbf{R}) \sim \exp(i\mathbf{K}_0 \cdot \mathbf{R}) \exp[-(\mathbf{R} - \mathbf{R}_0)^2/4\sigma^2]$  and the ground state of the relative motion Hamiltonian,  $\phi_0(r)$ . Note, however, that no separability is assumed during the propagation.

### 3. 1D potential ramp

Below we consider specifically the cases of a 1D potential ramp,  $U_{\text{ext}} = U_e(r_e) + U_h(r_h)$ , where  $U_{e(h)}(r_{e(h)}) = \mp ez_{e(h)}[(V_a - V_g) + (V_b - V_a)r_{e(h)}/(sL)]$ , generally used to accelerate the IXs along the QW plane in devices [see Fig. 1(a)-inset]. [6] This is somehow a special case, in that the c.m. and relative coordinates are separable, and  $U_{\text{ext}} = U_{\text{bias}} + U_{\text{c.m.}}^{\text{acc}}(R) + U_{\text{rel}}^{\text{acc}}(r)$ , where  $U_{\text{bias}} = ed(V_a - V_g)$  is a constant bias energy, which does not affect the dynamics, and  $U_{\text{c.m.}}^{\text{acc}}(R) = ed[(V_b - V_a)/(sL)]R$  is the c.m. accelerating potential. In a classical picture,  $U_{\text{c.m.}}^{\text{acc}}(R)$  accelerates the electron-hole dipole according to  $M\dot{R} = -\partial_R U_{\text{c.m.}}^{\text{acc}}(R) = -ed[(V_b - V_a)/(sL)]$ . Therefore, this case may serve as a test-bed of our calculations, since the classical and quantum dynamics of the c.m., given by  $\partial_{tt}^2[\langle R \rangle(t)]$ , should coincide according to Ehrenfest's theorem. The correspondence is shown in Fig. 1(a).

The potential  $U_{\text{rel}}^{\text{acc}}(r) = -e(z_e + dm_e/M)[(V_b - V_a)/(sL)]r$  induces excitations of the internal degree of freedom and oscillations around  $r = 0$ , which can be quantitatively analyzed in terms

of c.m.-averaged projections on the  $\phi_n$ 's,  $a_n(t) = \int |\int \phi_n^*(r)\Psi(\mathbf{R}, r; t)dr|^2 dR$ . Figure 1(b) shows the transfer of energy between the ground and first excited state, with minor contributions from other states. Pictorially, this corresponds to oscillations of the internal wave packet around  $r = 0$ . For external potentials which are sufficiently strong with respect to the Coulomb binding energy of the  $e$ - $h$  pair, direct, or tunneling-mediated dissociation is also possible [see Fig. 1(c)].<sup>2</sup>

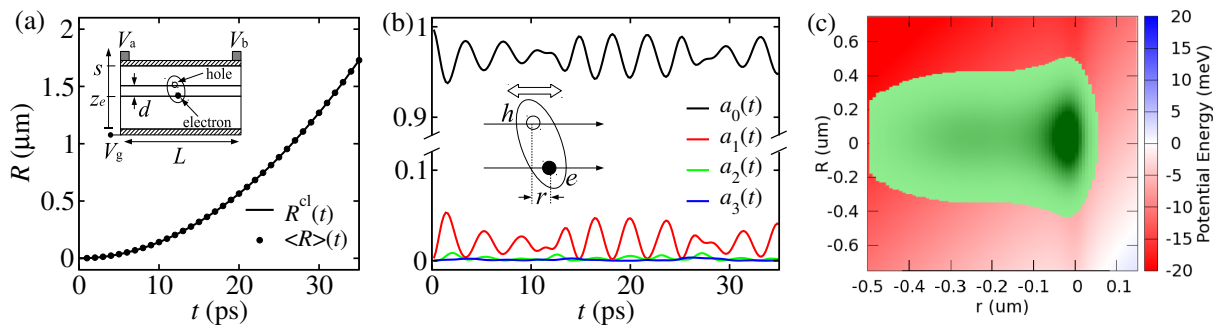


**Figure 1.** Propagation in a 1D potential ramp. (a) c.m. accelerated motion: classical (line) vs. Ehrenfest's (dots); inset: sketch of the physical system. (b) eigenstate population, showing the internal oscillating dynamics;  $\sigma = 150$  nm.  $d = 20$  nm,  $V_a - V_b = 0.5$  V. (c) snapshot of  $|\Psi(\mathbf{R}, r; t = 3 \text{ ps})|^2$  (green) together with total potential energy,  $U_{\text{int}} + U_{\text{ext}}$ ,  $U_{\text{int}}(r) = -1/(\epsilon\sqrt{r^2 + d^2})$ : example of dissociation in strong  $V_a - V_b = 1.5$  V.

#### 4. 2D potentials

We extend to 2D quantum wells the previous 1D model, and include non separable  $U_{\text{ext}}(\mathbf{R}, \mathbf{r})$ . Moreover, in order to have a more quantitative insight about the purely c.m. and internal dynamical correlations, and their effect on the IX propagation, we compare exact calculations with the so-called rigid exciton (RIX) model, in which the c.m. moves in the effective potential  $U_{\text{eff}}(\mathbf{R}) = \int d\mathbf{r} U_{\text{ext}}(\mathbf{R}, \mathbf{r}) |\phi_0(r)|^2$ , where  $U_{\text{ext}}$  is averaged on the internal motion ground state  $\phi_0(r)$ , in which the IX is supposed to be frozen. In these rigid-particle calculations, only the c.m. wave function  $\chi(\mathbf{R}; t)$  is propagated under  $U_{\text{eff}}(\mathbf{R})$ . On the contrary, in exact simulations, where *no specific form* on  $\Psi(\mathbf{R}, \mathbf{r}; t)$  is assumed, the problem is a full 4-DOF-dynamics. Here, a very large number of grid points is needed ( $\sim 2^{32}$  in typical 4-DOF-simulation), so it is essential to exploit massively parallel architectures.

To analyze results in 2D simulations we define the IX transmission  $T = \int_{\mathbf{T}} d\mathbf{R} \rho_{\text{c.m.}}(\mathbf{R}; t \rightarrow \infty)$ , i.e. the integral, over the region  $\mathbf{T}$  beyond the external potential [see inset in Fig.2(a)], of the c.m. marginal probability  $\rho_{\text{c.m.}}(\mathbf{R}; t) \equiv \int d\mathbf{r} |\Psi(\mathbf{R}, \mathbf{r}; t)|^2$  at asymptotic times. Note that in the RIX model  $\rho_{\text{c.m.}}(\mathbf{R})$  simply coincides with  $|\chi(\mathbf{R}; t)|^2$ .

We start considering the transmission of the IX wave packet in the scattering by a potential  $U_{\text{ext}} = U_{e,0}[\theta(y_e)\theta(L_y - y_e)]$ , with  $U_{e,0} < 0$ , i.e., an energy well for the electron alone, while the hole propagation is free, apart from Coulomb interaction [see Fig. 2(a)-inset]. This potential cannot be separated into the sum of c.m. and relative motion terms. The RIX model captures the full calculation results only when  $U_{e,0}$  is shallow, i.e. well below the first internal excitation energy,  $(\epsilon_1 - \epsilon_0) \approx 2.35$  meV.

As a second paradigmatic example, we simulate the IX scattering against a slit opened in a potential consisting of a barrier for the hole of height  $U_{h,0} = +6$  meV and an electron well of depth  $U_{e,0} = -3$  meV. As shown in Fig. 2(b-c), the shape of the exact diffraction patterns in transmission/reflection is not well reproduced by the RIX method. Moreover, the exact

<sup>2</sup> We use GaAs well in-plane effective masses  $m_e = 0.067 m_0$ ,  $m_h = 0.111 m_0$ , and dielectric constant  $\epsilon = 12.9$ .

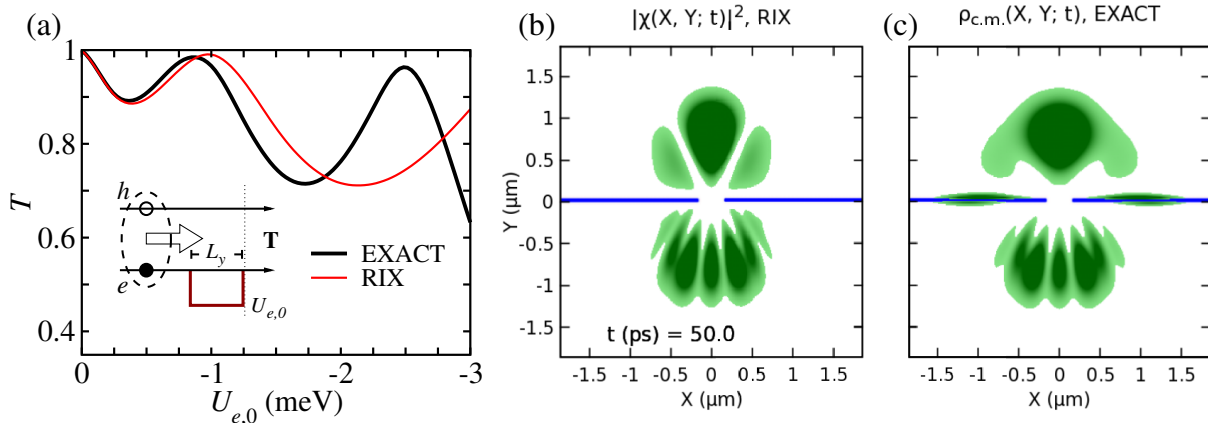


**Figure 2.** Results from 2D calculations, with initial c.m. kinetic energy of 0.4 meV. (a) Transmission  $T$  vs. electron well depth,  $U_{e,0}$ : (black) exact 4 DOF propagation; (red) RIX approximation. (a)–inset: sketch of the scattering;  $\sigma = 80$  nm.  $L_y = 40$  nm. (b–c) Scattering through a 240 nm-wide slit: snapshot at  $t = 50$  ps in RIX and exact models (see text for details);  $\sigma = 160$  nm.  $L_y = 20$  nm.

calculation exposes that a significant part of the IX wave packet moves along the edges of the external potential, a behaviour which can be explained as the Coulomb bound state of the electron, captured by its well, and the hole, confined outside its potential barrier. Being a purely two-particle dynamical process, this behaviour is not captured by RIX simulations.

## 5. Conclusions

We showed that both c.m. and internal quantum dynamics of a bound system must be taken into account in a wide variety of collisional phenomena. The rigid-particle approximation cannot account for most of pure two-body behaviours (excitations and dissociation of the bound state, diffraction patterns, etc.), which arise in real-time-and-space exact quantum propagations. Even more refined mean-field approximations allowing internal dynamics, but keeping the total wave function factorized, neglect – by construction – the correlation between c.m. and internal DOFs, and prove to fail in reproducing correct results.[1] Two-body phenomena quantitatively dictate transmission/reflection coefficients, and might be of fundamental importance in quantum device engineering.

## 6. Acknowledgments

We acknowledge the CINECA award under Iskra C project IsC33-FUQUDEX for computing time on parallel architectures.

## References

- [1] F Grasselli, A Bertoni, and G Goldoni 2016 *Phys. Rev. B* **93** 195310
- [2] M Suzuki 1993 *Proceedings of the Japan Academy, Series B* **69** 161
- [3] F Grasselli, A Bertoni, and G Goldoni 2015 *J. Chem. Phys.* **142** 034701
- [4] C Leforestier, R Bisseling, C Cerjan, M Feit, R Friesner, A Gulberg, A Hammerich, G Jolicard, W Karrlein, H-D Meyer, N Lipkin, O Roncero, and R Kosloff 1991 *J. Comput. Phys.* **94** 59
- [5] A Castro, M A L Marques, and A Rubio 2004 *J. Chem. Phys.* **121** 3425
- [6] A Gärtner, A W Holleitner, J P Kotthaus, D Schuh 2006 *Appl. Phys. Lett.* **89** 052108